Annals of R.S.C.B., ISSN:1583-6258, Vol. 25, Issue 3, 2021, Pages. 5573- 5588
Received 16 February 2021; Accepted 08 March 2021.

Non-conventional Method of Determination of Refractive Index using Fiber Optic U-shaped Glass Sensor in the Study of Certain Biological Fluids

Dr. S. Venkateswara Rao[1] & S. Srinivasulu[2*]

Corresponding Author: S. Srinivasulu[*] (siluverusrinivasulu@gmail.com)

[1]Professor of Physics, Department of Physics, College of Engineering Hyderabad, J N T University Hyderabad, Telangana State, India.

[2]UGC–Senior Research Fellow, Department of Physics, College of Engineering Hyderabad, J N T University Hyderabad, Telangana State, India.

ABSTRACT: Uniform U-shaped glass probe based extrinsic optical fiber refractive index sensors have tremendously received attention in the research and development across the world in the recent past. The U-bent probe as an extrinsic element in the design of optical fiber sensors provides the enhancement in the sensitivity at higher orders in the investigation of refractive index of various liquids including certain biological fluids. In the present work, the U-shaped probe with definite dimensions connected between a source of 660nm and a bench mark light detector, becomes a clad removed part of the sensor and acts as the sensing zone of the sensor. By immersing the glass rod into liquid mixtures of various indices of refraction, the power reaching the detector was recorded corresponding to the refractive index of liquid mixtures. Plotting the graph by taking refractive index on X-axis and power output on Y-axis a calibrated curve was drawn, which can be used to determine refractive index of various liquids including certain biological fluids. This method of measuring refractive index of liquids is a novel and nonconventional, which was completely different from the conventional methods which were popular in recent times of determination of refractive index of liquids.

Keywords: Calibrated curve, Definite dimensions, Nonconventional, Power output, Refractive index, Sensing zone, Uniform U-shaped glass probe.

INTRODUCTION

Recent progress of fiber optic sensors has brought a significant development in the measurement of refractive index of liquids in the latest past. The changes in the refractive index of liquids can be attributed to the scattering and absorption characteristics of light at the wavelengths of visible region. The development in the technology of optical fiber sensors has seen an exponential growth since 1960's due to intensive effort in the research with the combination of lasers and optical fibers. The low loss optical fibers were developed during 1970's and was exploited in optical fiber communications across the globe. But the phenomena of sensitivity of optical fibers for various external and internal perturbations made

Annals of R.S.C.B., ISSN:1583-6258, Vol. 25, Issue 3, 2021, Pages. 5573- 5588
Received 16 February 2021; Accepted 08 March 2021.

them to exploit to construct numerous measurement and sensing techniques to sense various environmental parameters. The Motivation towards optical fiber sensors can be attributed to several advantages of optical fibers over the conventional sensor technologies, that include portability, cost effectiveness, light weight, electrically passive nature, potential for multiplexing, capability of remote sensing, employability as OTDR and measurement of various parameters present in the radiation fields, etc. [1-3]. Optical fiber sensors either as an intrinsic sensor wherein the light is subjected to a modulation by the measurand or an extrinsic device wherein the light modulation takes place at the outside of the fiber medium have been exploited successfully in various designs to measure numerous environmental parameters [4]. To measure various biological, physical, mechanical, chemical and medicinal parameters, optical fiber sensors thus have been developed for monitoring chemical processes as chemical sensor, environmental condition monitoring, pollution related parameters, biosensors to monitor biological parameters, etc. For quantifying the refractive index in terms of concentration levels of several liquid solutions, the fiber optic chemical sensor is frequently employed as refractometer to determine refractive index of sucrose, acetonitrile, salt, dimethyl sulfoxide (DMSO), glycerol, methanol, etc. and as the refractive index of medium is temperature dependent, the sensor can be used to measure the temperature, in addition [5-10]. The replacement of fiber cladding with sensitized coating deposition on the surface, prepared by the Sol-Gel method enables to construct several sensors, which can be used to measure several environmental parameters at highest degree of accuracy and sensitivity [11-13]. The concentration of methane can be measured using this approach wherein cryptophane-E can be used as the sensitive coating in the region of clad removed portion, which acts as a sensing zone of the sensor. In the process of CH_4 measurement with the sensor, the variation induced in the refractive index of the cryptophane with respect to CH_4 concentration was measured and the sensor can be calibrated between refractive index and concentration of CH_4 [14]. By exploiting the various principles of operation such as tapering of optical fibers [15-18], employing end face Fresnel reflection using single mode fibers, interference among multi-modes [19-21], surface plasmon resonance [22-26], fiber Bragg gratings [27,28], LPGs [29], etc. for the measurement of refractive index. In a further design, a cost-effective, simple, miniaturized, quick response sensor can be designed by using a partially or totally stripped off cladding fiber used at the region of sensing employing multimode fibers to detect the refractive index of various substances [30-34].

Propagation of laser beam in multimode optical fibers takes place by innumerable number of total internal reflections (TIR) by fulfilling the Snell's law at core-cladding interface with a critical angle of "θ_c" expressed as

$$\theta_c = \sin^{-1}\left[\frac{n_{cl}}{n_{co}}\right]$$

Annals of R.S.C.B., ISSN:1583-6258, Vol. 25, Issue 3, 2021, Pages. 5573- 5588
Received 16 February 2021; Accepted 08 March 2021.

Where: n_{cl} – Refractive index of the cladding

n_{co} – Refractive index of the core

In multimode fibers all the modes, whose incident angle lies between "θ_c" and "90^o" at core-cladding interface only propagate through the fiber subjected to TIR, where as in single mode fibers only single mode can propagate through the fiber for which the required size of the core lies between 5–10µm. The number of modes propagating through step index multimode fibers can be expressed in terms of "V" number (normalized frequency) as

$$M = \frac{V^2}{2}$$

Assigning various values to "V" number, it is possible to define whether a particular fiber is a multimode fiber or a single mode fiber. For "V" > 2.405, the fiber supports numerous modes and acts as a multimode fiber and for "V" < 2.405, the fiber supports only one mode called as single mode fiber. The normalized frequency can be influenced by core radius of the fiber (a), refractive index of the core (n_{co}), refractive index of the cladding (n_{cl}) and the operational wavelength (λ) of the light launched into the fiber as

$$V = \frac{2\pi a}{\lambda}\sqrt{n_{co}^2 - n_{cl}^2}$$

$$V = \frac{2\pi a}{\lambda}(NA)$$

Where: NA – Numerical aperture = $\sqrt{n_{co}^2 - n_{cl}^2}$

EXPERIMENTAL DETAILS

In the design of the sensor, two 200/230µm multimode PCS fibers were connected to the U-shaped glass rod, the other end of the first fiber is connected to a light source of 660nm operational wavelength at the transmitter end and the other end of the second fiber is connected to a benchmark power meter at the receiver end. In order to calibrate the sensor between the parameters of refractive index and the output power, a series of solutions using toluene and water were prepared using a two burette arrangement. Solutions with different refractive index values are prepared by taking the water and toluene in different proportions making the total volume of the solution equivalent to 20ml, the solutions are taken in different glass containers using air tight lids and preserved them for the experimentation.

Annals of R.S.C.B., ISSN:1583-6258, Vol. 25, Issue 3, 2021, Pages. 5573- 5588
Received 16 February 2021; Accepted 08 March 2021.

Table.1: Standard properties of Toluene and Water.

Properties	**Toluene (C_7H_8)**	**Water (H_2O)**
Structure:	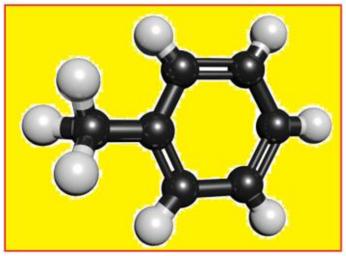	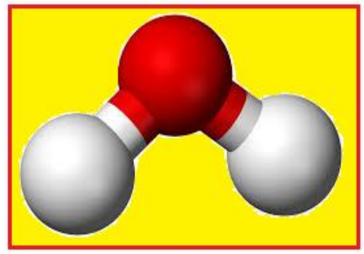
CAS Number:	108-88-3	7732-18.5
Molar Mass (g/mole):	92.141	18.02
Density (kg/m^3):	0.8697×10^3 at 20^oC	0.9982×10^3 at 20^oC
Colour:	Colourless	Colourless
Refractive index:	1.4967 at 20^oC	1.3330 at 20^oC
Melting point:	-94.9^oC	0^oC
Boiling point:	110.6^oC	100^oC

The research work has been carried out taking three aspects into consideration.

1. Investigation of refractive index variation corresponding to the output power variation at room temperature.
2. Study of variation in output power with respect to the corresponding temperature dependent variation of refractive index of liquid solution between 10^oC to 60^oC.
3. Calibration of the sensor based on the length of the liquid cladding at the region of sensing.

Calculation of mole fraction:

The properties of binary solutions significantly changes on the presence of number of solute particles in the resultant solution. The refractive index variations of solutions, thus depends upon the amount of solute particles in the solution. In the present study the water has been taken as a solute and the toluene was taken as solvent liquid. Therefore, the solutions with different proportions and with specific ratios were added to prepare the solution of toluene and water, making the total volume as 20ml. Thus, the different ratios of solutions are prepared by taking toluene (ml) : water(ml) → (20:0), (18:2), (16:4), (14:6), (12:8), (10:10), (8:12), (6:14), (4:16), (2:18), (0:20) to calibrate the sensor. The mole fractions of solute liquid in the solution can mathematically be determined using the following expression.

$$\text{Mole Fraction } (X_1) = \frac{\text{Number of moles of substance} - 1}{\text{Total number of moles}}$$

$$\text{Mole Fraction } (\mathrm{X}_1) = \frac{\text{Number of moles of substance} - 1}{\text{Number of moles of substance} - 1 + \text{Number of moles of substance} - 2}$$

$$\text{Number of moles} = \frac{\text{Mass of substance}}{\text{Mass of one mole substance}}$$

$$\text{Density} = \frac{\text{Mass}}{\text{Volume}}\text{ ; Mass} = \text{Density} \times \text{Volume}$$

Annals of R.S.C.B., ISSN:1583-6258, Vol. 25, Issue 3, 2021, Pages. 5573- 5588
Received 16 February 2021; Accepted 08 March 2021.

$$\text{Number of moles} = \frac{\text{Volume} \times \text{Density}}{\text{Molar mass}}$$

$$X_1 = V_1(\rho_1/M_1)$$

$$\therefore \text{Mole Fraction } (X_1) = \frac{V_1(\rho_1/M_1)}{V_1(\rho_1/M_1)+V_2(\rho_2/M_2)}$$

Where: M_1, M_2: Molecular weights of chemicals (kg.mole^{-1})

ρ_1, ρ_2: Densities of chemicals (kg.m^{-3})

V_1, V_2: Volumes of chemicals (liters)

Determination of refractive index of solutions at various temperatures:

Automatic digital refractometer of modal number RX-7000i (Atago make, Japan) operating at the wavelength of 5893Å capable of operating up to 70^{o}C, was employed to determine the refractive indices of all the liquid solutions between the temperatures from 10^{o}C to 60^{o}C. Taking a small quantity of liquid from each solution and raising the temperature of the device form 10^{o}C to 60^{o}C, the refractive index of all the solutions at different temperatures in steps of 5^{o}C each was recorded and tabulated.

Table.2: Mole fraction of Water in Toluene + Water solution and Refractive indices of solution at various temperatures (from 10^{o}C to 60^{o}C).

S. No.	Mole fraction of Water	Refractive Index at various temperatures										
		10^{o}C	15^{o}C	20^{o}C	25^{o}C	30^{o}C	35^{o}C	40^{o}C	45^{o}C	50^{o}C	55^{o}C	60^{o}C
1	0.00000	1.50915	1.50591	1.50171	1.4977	1.49325	1.48974	1.48582	1.48293	1.47795	1.47509	1.47102
2	0.39502	1.44304	1.4395	1.43609	1.43299	1.43012	1.42714	1.42423	1.42104	1.41873	1.41584	1.41227
3	0.59501	1.41109	1.40823	1.40523	1.40214	1.39897	1.39517	1.39204	1.38908	1.38614	1.38352	1.38009
4	0.71579	1.39248	1.38908	1.38614	1.38305	1.37959	1.37708	1.37415	1.37009	1.36798	1.36541	1.36235
5	0.79665	1.37832	1.37504	1.37205	1.36921	1.36675	1.36341	1.36082	1.35701	1.35457	1.35108	1.34814
6	0.85458	1.36921	1.36598	1.36307	1.36007	1.35701	1.35405	1.35152	1.34855	1.34483	1.34207	1.33899
7	0.89811	1.36207	1.35914	1.35615	1.35325	1.35006	1.34714	1.34445	1.34161	1.33831	1.33552	1.33208
8	0.93203	1.35652	1.35325	1.35032	1.34751	1.34483	1.34207	1.33941	1.33632	1.33316	1.33004	1.32617
9	0.95919	1.35204	1.34904	1.34599	1.34344	1.34044	1.33732	1.33442	1.33128	1.32804	1.32489	1.32197
10	0.98144	1.34714	1.34413	1.34124	1.33831	1.33503	1.33208	1.32956	1.32617	1.32326	1.32004	1.31743
11	1.00000	1.34298	1.34006	1.33732	1.33403	1.33089	1.32721	1.32425	1.32107	1.31804	1.31508	1.31252

Measurement of output power at different temperatures for a depth of immersion of glass rod into the liquid solution equal to 1cm, 2cm and 3cm:

The length of interaction of measurer (light) with measurand (liquid solution) greatly influences the absorption of light at the region of sensing and hence power reaching the output end. Greater the length of interaction between light and liquid at the sensing zone, smaller the output power reaching the detector.

The power absorption, at the region of sensing also influenced by the radius of curvature of macro bend and thickness of the glass rod. Thus, in the present study the loss of light depends on

1. Length of interaction of light with the liquid cladding.
2. Radius of curvature of macro-bend of the U-shaped glass rod
3. Thickness of the U-shaped glass rod
4. Absorbing nature of the liquid cladding.

The study has been carried out by fixing the thickness of the glass rod and radius of curvature of macro-bend, but by changing the interaction length between light travelling through glass rod and liquid cladding as 1 cm, 2 cm, & 3 cm. The experimentation was initiated by selecting the depth of immersion of U-shaped glass rod into liquid as 1cm and measuring the output power reaching the detector. The glass rod is connected between the source and detector was immersed to a depth of 1cm into the first solution and power reaching the detector was recorded at various temperatures by heating the solutions by using a special temperature bath, capable of varying temperature from 10°C to 60°C. This method of recording the output power was repeated for 2cm and 3cm of immersions of U-shaped glass rod and for using other ratios of solutions [Tables: 3 – 5].

Table.3: Mole fraction of Water in Toluene + Water solution and Output power at various temperatures (from 10°C to 60°C), when depth of immersion of U-shaped glass rod into chemical mixture is 1cm.

Output Power when air surrounding the U-shaped glass rod: -24.80dBm (at 30°C)

S. No.	Mole fraction of Water	Output Power(dBm) at various temperatures										
		10°C	15°C	20°C	25°C	30°C	35°C	40°C	45°C	50°C	55°C	60°C
1	0.00000	-39.50	-39.20	-38.90	-38.57	-38.23	-38.00	-37.63	-37.47	-37.10	-36.83	-36.53
2	0.39502	-34.70	-34.50	-34.20	-34.00	-33.77	-33.50	-33.33	-33.10	-32.87	-32.70	-32.47
3	0.59501	-32.33	-32.20	-31.90	-31.70	-31.43	-31.17	-30.90	-30.63	-30.40	-30.17	-29.90
4	0.71579	-30.93	-30.63	-30.40	-30.10	-29.87	-29.67	-29.47	-29.13	-29.00	-28.80	-28.60
5	0.79665	-29.77	-29.53	-29.30	-29.07	-28.90	-28.67	-28.47	-28.13	-27.93	-27.67	-27.43
6	0.85458	-29.07	-28.83	-28.63	-28.40	-28.13	-27.90	-27.70	-27.47	-27.13	-26.93	-26.73
7	0.89811	-28.57	-28.33	-28.07	-27.83	-27.57	-27.33	-27.10	-26.90	-26.70	-26.60	-26.37
8	0.93203	-28.10	-27.83	-27.60	-27.37	-27.13	-26.93	-26.77	-26.63	-26.43	-26.23	-25.97
9	0.95919	-27.73	-27.50	-27.23	-27.03	-26.83	-26.67	-26.53	-26.33	-26.10	-25.90	-25.70
10	0.98144	-27.33	-27.07	-26.87	-26.70	-26.57	-26.37	-26.20	-25.97	-25.80	-25.57	-25.43
11	1.00000	-27.00	-26.80	-26.67	-26.50	-26.30	-26.03	-25.87	-25.63	-25.47	-25.30	-25.13

Table.4: Mole fraction of Water in Toluene + Water solution and Output power at various temperatures (from 10°C to 60°C), when depth of immersion of U-shaped glass rod into chemical mixture 2cm.

Annals of R.S.C.B., ISSN:1583-6258, Vol. 25, Issue 3, 2021, Pages. 5573- 5588
Received 16 February 2021; Accepted 08 March 2021.

Output Power when air surrounding the U-shaped glass rod: -24.80dBm (at 30°C)

S. No.	Mole fraction of Water	Output Power(dBm) at various temperatures										
		10°C	15°C	20°C	25°C	30°C	35°C	40°C	45°C	50°C	55°C	60°C
1	0.00000	-42.20	-41.90	-41.50	-41.20	-40.80	-40.50	-40.13	-39.83	-39.40	-39.13	-38.83
2	0.39502	-36.50	-36.20	-35.90	-35.60	-35.33	-34.97	-34.70	-34.43	-34.23	-33.97	-33.63
3	0.59501	-33.47	-33.27	-32.97	-32.73	-32.43	-32.17	-31.90	-31.67	-31.43	-31.20	-30.87
4	0.71579	-31.93	-31.67	-31.43	-31.13	-30.83	-30.63	-30.37	-29.97	-29.77	-29.53	-29.27
5	0.79665	-30.73	-30.43	-30.17	-29.90	-29.67	-29.37	-29.13	-28.77	-28.57	-28.33	-28.13
6	0.85458	-29.90	-29.60	-29.33	-29.03	-28.77	-28.53	-28.37	-28.17	-27.90	-27.70	-27.47
7	0.89811	-29.23	-28.97	-28.70	-28.47	-28.27	-28.07	-27.87	-27.67	-27.43	-27.23	-27.03
8	0.93203	-28.73	-28.47	-28.30	-28.10	-27.90	-27.70	-27.50	-27.30	-27.10	-26.90	-26.63
9	0.95919	-28.40	-28.20	-27.97	-27.80	-27.57	-27.37	-27.17	-27.00	-26.77	-26.57	-26.37
10	0.98144	-28.07	-27.83	-27.63	-27.43	-27.20	-27.03	-26.87	-26.63	-26.47	-26.23	-26.07
11	1.00000	-27.77	-27.53	-27.37	-27.13	-26.97	-26.70	-26.53	-26.30	-26.10	-25.90	-25.70

Table.5: Mole fraction of Water in Toluene + Water solution and Output power at various temperatures (from 10°C to 60°C), when depth of immersion of U-shaped glass rod into chemical mixture 3cm.

Output Power when air surrounding the U-shaped glass rod: -24.80dBm (at 30°C)

S. No.	Mole fraction of Water	Output Power(dBm) at various temperatures										
		10°C	15°C	20°C	25°C	30°C	35°C	40°C	45°C	50°C	55°C	60°C
1	0.00000	-45.23	-44.87	-44.47	-44.07	-43.63	-43.27	-42.87	-42.57	-42.03	-41.80	-41.40
2	0.39502	-38.80	-38.37	-38.10	-37.70	-37.47	-37.20	-36.87	-36.63	-36.37	-36.13	-35.80
3	0.59501	-35.63	-35.27	-35.03	-34.70	-34.43	-34.03	-33.63	-33.30	-32.97	-32.73	-32.33
4	0.71579	-33.70	-33.30	-32.97	-32.67	-32.27	-32.03	-31.77	-31.33	-31.13	-30.87	-30.57
5	0.79665	-32.17	-31.83	-31.53	-31.27	-31.00	-30.67	-30.43	-30.07	-29.90	-29.63	-29.30
6	0.85458	-31.27	-30.93	-30.63	-30.37	-30.07	-29.87	-29.67	-29.33	-28.97	-28.70	-28.37
7	0.89811	-30.53	-30.27	-30.00	-29.80	-29.53	-29.17	-28.93	-28.63	-28.30	-28.07	-27.87
8	0.93203	-30.03	-29.80	-29.57	-29.23	-28.97	-28.70	-28.40	-28.13	-27.93	-27.67	-27.33
9	0.95919	-29.70	-29.40	-29.07	-28.83	-28.53	-28.20	-28.00	-27.80	-27.50	-27.23	-27.00
10	0.98144	-29.17	-28.87	-28.60	-28.30	-28.03	-27.87	-27.63	-27.33	-27.10	-26.83	-26.63
11	1.00000	-28.77	-28.47	-28.20	-27.97	-27.77	-27.43	-27.20	-26.93	-26.67	-26.43	-26.23

RESULTS AND DISCUSSION

The refractive index of liquid defines the speed of light in vacuum by speed of speed of light in the liquid (medium). The refractive index of medium depends on the polarizing nature of the medium, either it can

Annals of R.S.C.B., ISSN:1583-6258, Vol. 25, Issue 3, 2021, Pages. 5573- 5588
Received 16 February 2021; Accepted 08 March 2021.

be in the state of gas, liquid or solid. More are the presence of atoms having more polarizing nature, greater is the refractive index. Therefore, the presence of mole fraction of solute i.e. water in solution of toluene + water, changes the refractive index of the solution drastically effecting the speed of the light and resulting heavy absorption of light at the region of sensing. The influence of mole fraction of water corresponding change in the refractive index is presented graphically [fig.-1].

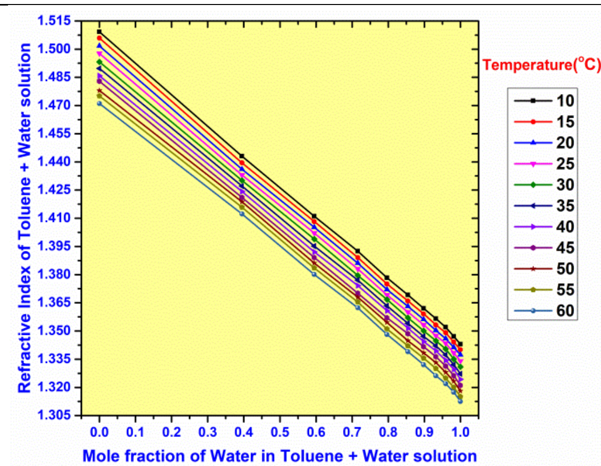

Fig.1: Relation between Mole fraction of Water in Toluene + Water solution and Refractive index.

The presence of water in the solution of toluene + water similarly decides the concentration of the solution. From the data obtained for variation in refractive index of toluene + water solution with respect to concentration percentage of water in toluene + water solution was presented in graph [fig.-2].

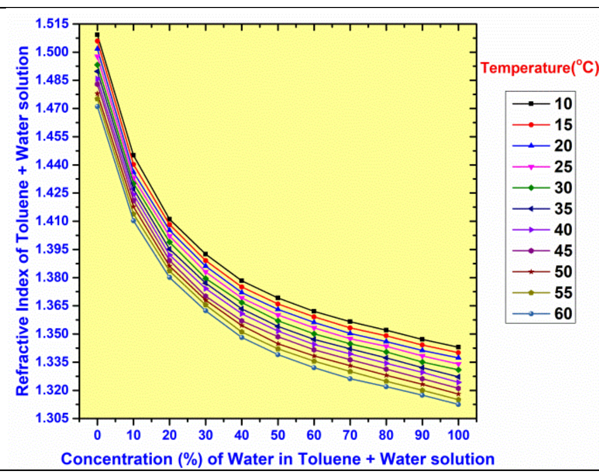

Fig.2: Relation between Concentration (%) of Water in Toluene + Water solution and Refractive index.

The refractive index of solution decreases exponentially with increase in the concentration percentage of water in toluene + water solution. Refractive index of solution is temperature dependent variable, and the

Annals of R.S.C.B., ISSN:1583-6258, Vol. 25, Issue 3, 2021, Pages. 5573- 5588
Received 16 February 2021; Accepted 08 March 2021.

relation between the refractive index variation with respect to temperature was recorded graphically [fig.-3].

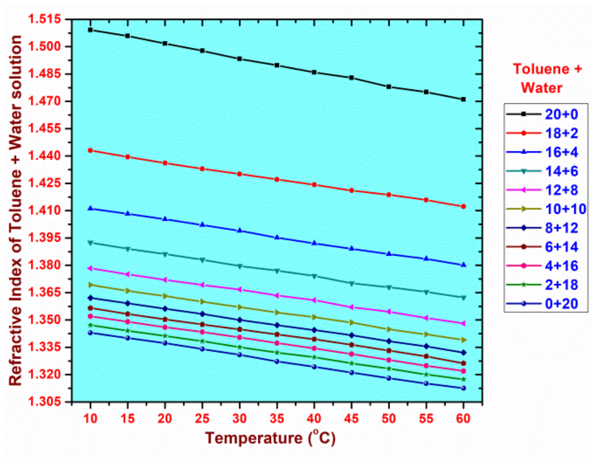

Fig.3: Relation between Temperature and Refractive index of Toluene + Water solution.

As the mole fraction of the solute in the solution increases, the refractive index decreases and as the temperature increases, the refractive index decreases, and thus as these three parameters depends on one another a 3dimentional graph is plotted to show their dependent variation on one another [fig.-4].

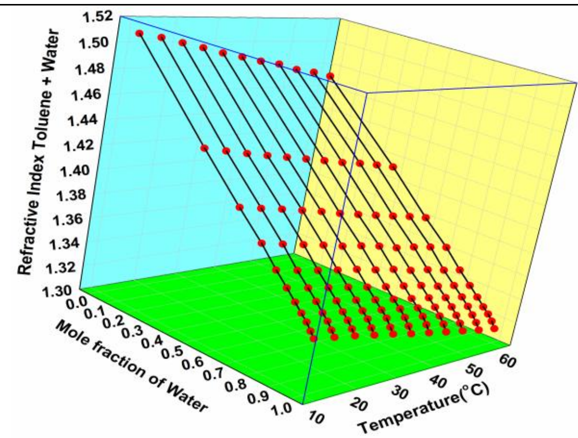

Fig.4: Relation among Mole fraction of Water in Toluene + Water solution, Refractive index and Temperature.

The concentration of solute particles increases in the solution, the refractive index decreases, and as the refractive index is temperature dependent variable, increase in the temperature, decreases the refractive index. The resultant variations of concentration, refractive index and temperature on one another were presented in the form of a 3dimentional graph [fig.-5].

Annals of R.S.C.B., ISSN:1583-6258, Vol. 25, Issue 3, 2021, Pages. 5573- 5588
Received 16 February 2021; Accepted 08 March 2021.

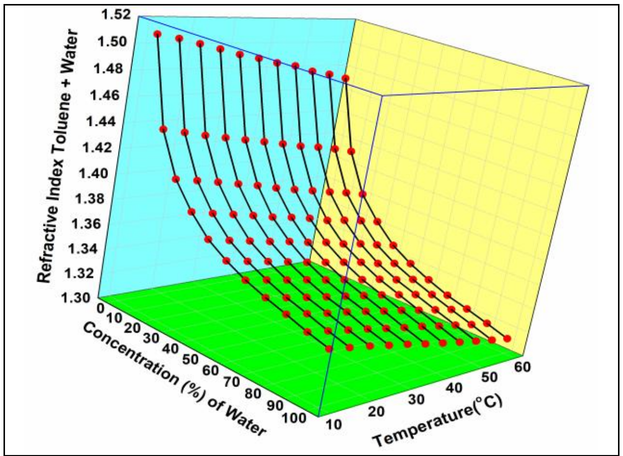

Fig.5: Relation among Concentration (%) of Water in Toluene + Water solution, Refractive index and Temperature.

The data generated for output power corresponding to the change in the mole fraction of solute in the solution for depths of immersions 1cm, 2cm and 3cm was used to plot graphs to present their variations on one another [fig.6-8].

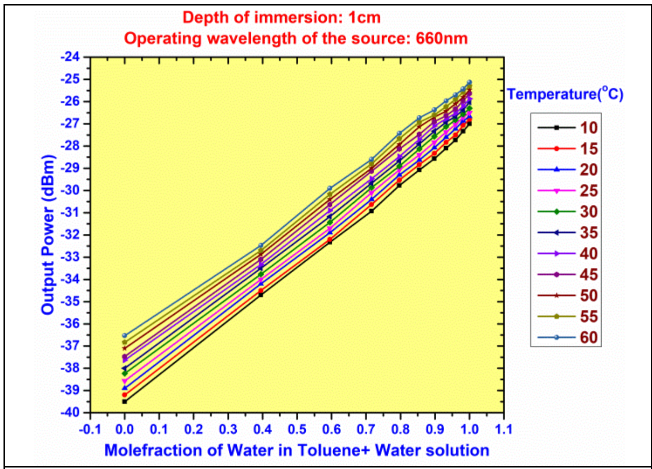

Fig.6: Relation between Mole fraction of Water in Toluene + Water solution and Output power at depth of immersion is 1cm.

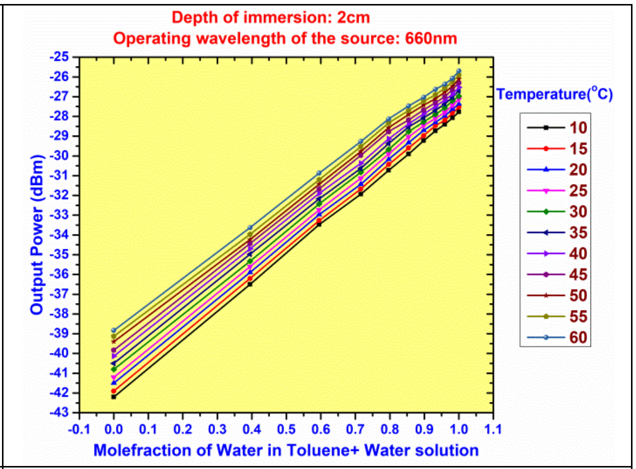

Fig.7: Relation between Mole fraction of Water in Toluene + Water solution and Output power at depth of immersion is 2cm.

Annals of R.S.C.B., ISSN:1583-6258, Vol. 25, Issue 3, 2021, Pages. 5573- 5588
Received 16 February 2021; Accepted 08 March 2021.

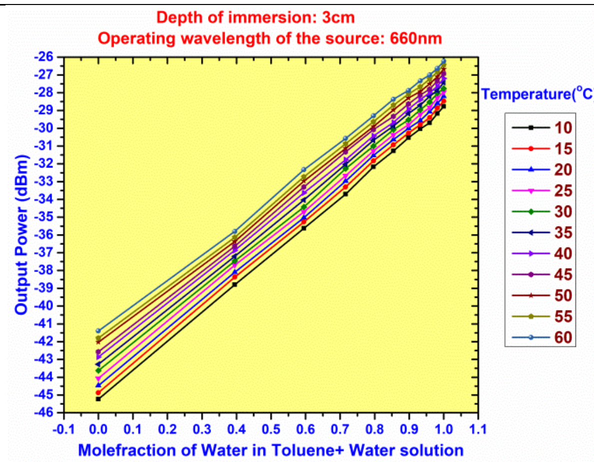

Fig.8: Relation between Mole fraction of Water in Toluene + Water solution and Output power at depth of immersion is 3cm.

The raise in the temperature of the liquid solution, decrease the refractive index of solution and hence increases the output power. This observation was studied at the depths of immersions of 1cm, 2cm and 3cm and presented in graphs [fig.9-11].

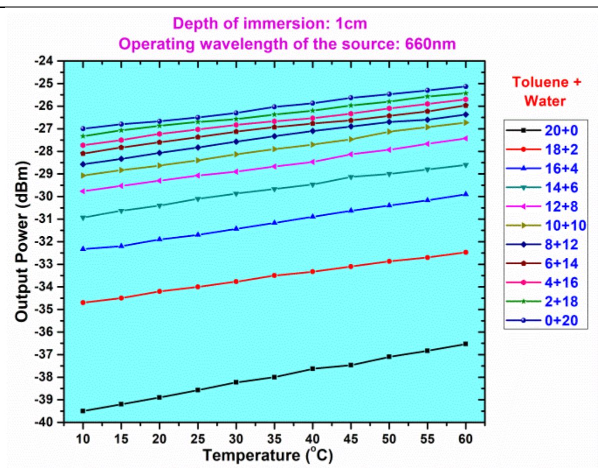

Fig.9: Relation between Temperature and Output power of Toluene + Water solution at depth of immersion is 1cm

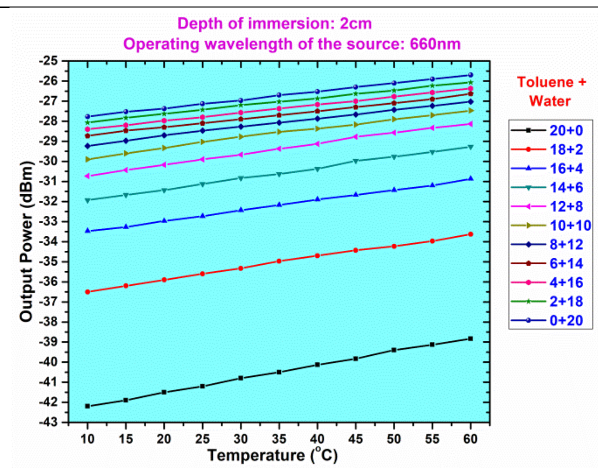

Fig.10: Relation between Temperature and Output power of Toluene + Water solution at depth of immersion is 2cm

Annals of R.S.C.B., ISSN:1583-6258, Vol. 25, Issue 3, 2021, Pages. 5573- 5588
Received 16 February 2021; Accepted 08 March 2021.

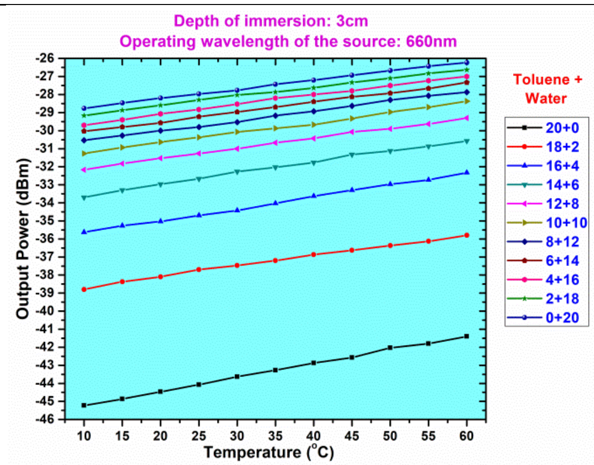

Fig.11: Relation between Temperature and Output power of Toluene + Water solution at depth of immersion is 3cm

The light travelling through the fiber, transmits unattenuated during first fiber leg and also second fiber leg. But at the region of sensing i.e. during its travel through the U-shaped glass rod it attenuates into the liquid solution as an evanescent wave due to bending of the rod, thickness of the rod and also due to length of interaction of light with the liquid cladding in the region of sensing. The higher order modes of the light are greatly affected by the above three parameters and will be absorbed by the liquid cladding. More is increase in the refractive index of the liquid cladding, more are the absorption of the higher order modes and hence more is the loss of light. Thus, the fewer amounts of power reaching the detector, but as the refractive index is temperature dependent variable, the raise in the temperature decrease the refractive index and resulting the corresponding increase in the output power at the receiver end. This variation of light increase at the output end, varying with different depth of immersion of 1cm, 2cm and 3cm resulting graphs are shown in figures [fig.12-14].

Annals of R.S.C.B., ISSN:1583-6258, Vol. 25, Issue 3, 2021, Pages. 5573- 5588
Received 16 February 2021; Accepted 08 March 2021.

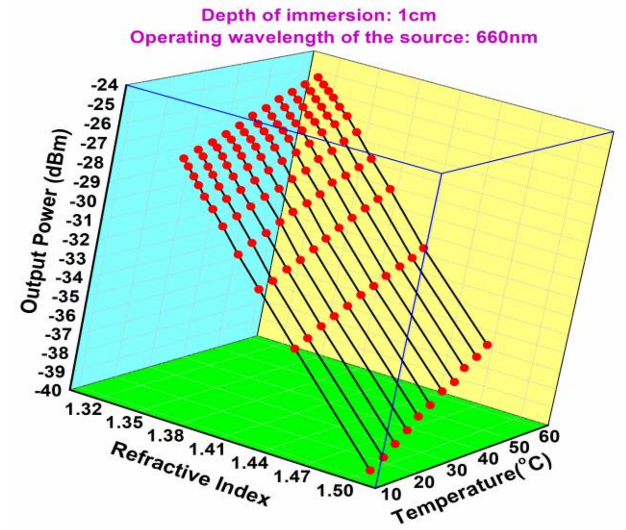

Fig.12: Relation between Refractive index, Output Power and Temperature of Toluene + Water solution at depth of immersion is 1cm

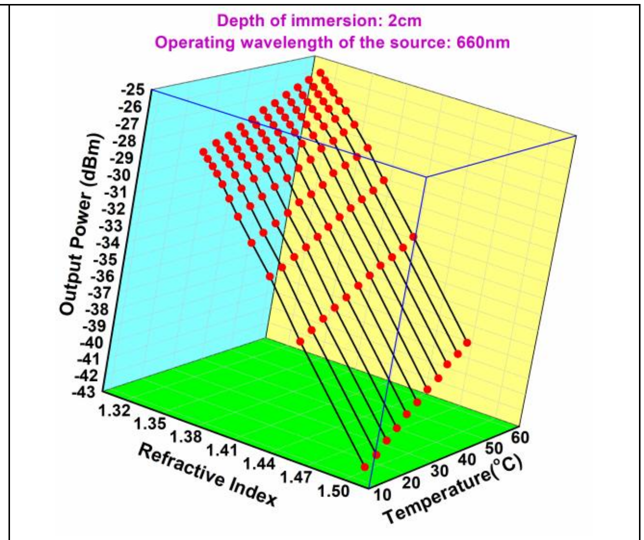

Fig.13: Relation between Refractive index, Output Power and Temperature of Toluene + Water solution at depth of immersion is 2cm

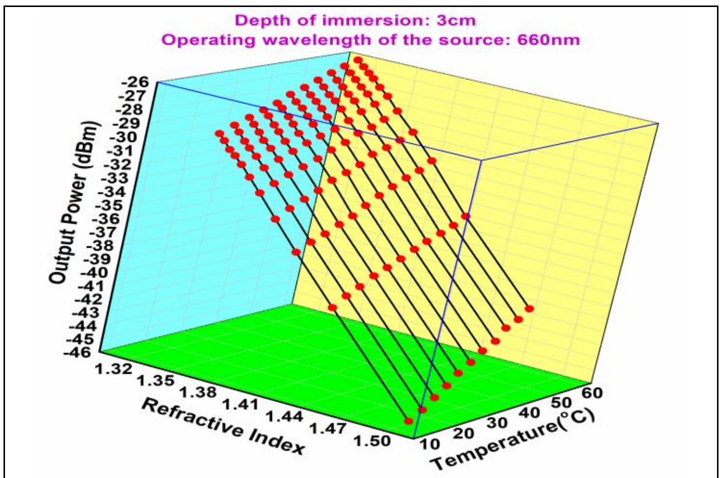

Fig.14: Relation between Refractive index, Output Power and Temperature of Toluene + Water solution at depth of immersion is 3cm

CONCLUSION

In the present study a fiber optic extrinsic sensor based on a U-shaped glass element proposed to be calibrated between refractive index and output power, working at the dynamic range of temperature between 10°C to 60°C. Toluene with high index of refraction (1.49325n_D at 30°C) and the water of low index of refraction (1.33089n_D at 30°C) was selected for the study of calibration of the sensor, operating in the dynamic range of refractive index between 1.50915n_D and 1.31252n_D at wavelength of sodium light. A temperature bath capable of raising the temperature from 10°C to 60°C and automatic digital refractometer of modal RX-7000i were employed to raise the temperature of liquid solution from 10°C to

Annals of R.S.C.B., ISSN:1583-6258, Vol. 25, Issue 3, 2021, Pages. 5573- 5588
Received 16 February 2021; Accepted 08 March 2021.

$60^{o}C$ and to record the refractive index of solutions respectively. Output powers were recorded corresponding to different temperatures and concentrations of liquids and at different depths of immersions of glass rod as 1cm, 2cm and 3cm. Calibrated curves are drawn among refractive index, temperature and output power which can be used to determine the refractive indices of various liquids including bio-fluids in the dynamic temperature range of $10^{o}C$ to $60^{o}C$ and refractive index range of $1.50915n_D$ to $1.31252n_D$.

REFERENCES

[1] Kersey, A. D. A review of recent developments in fber optic sensor technology. J. Opt. Fiber Tech. 2, 291–317 (1996).

[2] Grattan, K. T. V. & Sun, T. Fiber optic sensor technology: an overview. Sensors and Actuators A 82, 40–61 (2000).

[3] Lee, B. Review of the present status of optical fber sensors. J. Opt. Fiber Tech. 9, 57–79 (2003).

[4] Norris, J. O. W. Optical fber chemical sensors: fundamentals and applications in Optical Fiber Sensor Technology. (eds Grattan, K. T. V. & Meggitt, B. T.) 337–375 (Springer Science+Business Media, 2000).

[5] Abbate, G., Bernini, U., Ragozzino, E. & Somma, F. Te temperature dependence of the refractive index of water. J. Phys. D: Appl. Phys. 11, 1167–1172 (1978).

[6] Hu, T., Zhao, Y. & Song, A. Fiber optic SPR sensor for refractive index and temperature measurement based on MMF-FBG-MMF structure. Sensors and Actuators B 237, 521–525 (2016).

[7] Xu, W., Huang, X. G. & Pan, J. S. Simple fber-optic refractive index sensor based on fresnel refection and optical switch. IEEE Sensors J. 13, 1571–1574 (2013).

[8] Saunders, J. E., Sanders, C., Chen, H. & Loock, H. P. Te refractive index of common solvents and solutions at 1550 nm. Appl. Opt. 55, 947–953 (2016).

[9] Yang, N., Qiu, Q., Su, J. & Shi, S. Research on the temperature characteristics of optical fber refractive index. Int. J. Light. Electron Opt. 125, 5813–5815 (2014).

[10] Valkai, S., Liszi, J. & Szalai, I. Temperature dependence of the refractive index for three chloromethane liquids at 514.5 nm and 632.8 nm wavelengths. J. Chem. Termodynamics 30, 825–832 (1998).

[11] MacCraith, B. D., Ruddy, V., Potter, C., O'Kelly, B. & McGilp, J. F. Optical waveguide sensor using evanescent wave excitation of fuorescent dye in sol-gel glass. Electron. Lett. 27, 1247–1248 (1991).

[12] Badini, G. E., Grattan, K. T. V., Palmer, A. W. & Tseung, A. C. C. Development of pH-sensitive substrates for optical sensor applications application. Springer Proc. In Physics Berlin 44, 436 (1989).

[13] Shibata, S. Sol-gel-derived silica preforms for optical fbers. J. Non-Crystalline Solids 178, 272–283 (1994).

[14] Benounis, M., Jafrezic-Renault, N., Dutastab, J.-P., Cherif, K. & Abdelghani, A. Study of evanescent wave optical fbre sensor for methane detection based on cryptophane molecules. Sensors and Actuators B 107, 32–39 (2005).

[15] Villatoro, J., Monzón-Hernández, D. & Talavera, D. High resolution refractive index sensing with cladded multimode tapered optical fbre. Electron. Lett. 40, 106–107 (2004).

[16] Yadav, T., Narayanaswamy, K. R., Abu Bakar, M. H., Kamil, Y. M. & Mahdi, M. A. Single mode tapered fber-optic interferometer based refractive index sensor and its application to protein sensing. Opt. Express 22, 22802–22807 (2014).

[17] Wan, N. H. et al. High-resolution optical spectroscopy using multimode interference in a compact tapered fbre. Nat. Commun. 6, 7762, https://doi.org/10.1038/ncomms8762 (2015).

[18] Wong, Y. M., Scully, P. J., Kadim, H. J., Alexiou, V. & Bartlett, R. J. Automation and dynamic characterization of light intensity with applications to tapered plastic optical fbre. J. Opt. A: Pure Appl. Opt. 5, S51–S58 (2003).

[19] Fukano, H., Aiga, T. & Taue, S. High-sensitivity fber-optic refractive index sensor based on multimode interference using small-core single-mode fber for biosensing. Jpn. J. Appl. Phys. 53, (04EL08-1)–(04EL08-4) (2014).

[20] Li, Y., Liu, Z. & Jian, S. Multimode interference refractive index sensor based on coreless fber. Photonic Sensors 4, 21–27 (2014).

[21] Fukano, H., Hashimoto, T. & Taue, S. Refection-type optical fber refractive-index sensor using a multimode interference structure with high sensitivity. Jpn. J. Appl. Phys. 53, (04EG05-1)–(04EG05-4) (2014).

[22] Mishra, A. K., Mishra, S. K. & Gupta, B. D. SPR based fber optic sensor for refractive index sensing with enhanced detection accuracy and fgure of merit in visible region. Opt. Comm. 344, 86–91 (2015).

[23] Al-Qazwini, Y. et al. Refractive index sensor based on SPR in symmetrically etched plastic optical fbers. Sensors and Actuators A 246, 163–169 (2016).

[24] Mishra, S. K., Zou, B. & Chiang, K. S. Surface-Plasmon-Resonance Refractive-Index Sensor With Cu-Coated Polymer Waveguide. IEEE Photon. Technol. Lett. 28, 1835–1838 (2016).

[25] Ji, L. et al. Surface plasmon resonance refractive index sensor based on ultraviolet bleached polymer waveguide. Sensors and Actuators B 244, 373–379 (2017).

[26] Lin, Y.-C. Characteristics of optical fber refractive index sensor based on surface plasmon resonance. Microwave Opt. Technol. Lett. 55, 574–576 (2013).

[27] Wu, Q. et al. Fiber refractometer based on a fber Bragg grating and single-mode-multimode-single-mode fber structure. Opt. Lett. 36, 2197–2199 (2011).

Annals of R.S.C.B., ISSN:1583-6258, Vol. 25, Issue 3, 2021, Pages. 5573- 5588
Received 16 February 2021; Accepted 08 March 2021.

[28] Liang, W., Huang, Y., Xu, Y., Lee, R. & Kand, A. Yariv. Highly sensitive fber Bragg grating refractive index sensors. Appl. Phys. Lett. 86, 151122, https://doi.org/10.1063/1.1904716 (2005).

[29] Swart, P. L. Long-period grating Michelson refractometric sensor. Meas. Sci. Technol. 15, 1576–1580 (2004).

[30] Apriyanto, H. et al. A multimode fber refractive index sensor. Proc. IEEESensors 2016, 277–279, 30 Oct.- 2 Nov., Orlando, USA (2016).

[31] Liu, G. & Feng, D. Evanescent wave analysis and experimental realization of refractive index sensor based on D-shaped plastic optical fber. J. Light. Electron Opt. 127, 690–693 (2016).

[32] Sequeira, F. Refractive index sensing with d-shaped plastic optical fbers for chemical and biochemical applications. Sensors 16, 2119, https://doi.org/10.3390/s16122119 (2016).

[33] Banerjee, A. et al. Fiber optic sensing of liquid refractive index. Sensors and Actuators B 123, 594–605 (2007).

[34] De-Jun, F., Mao-Sen, Z., Liu, G., Xi-Lu, L. & Dong-Fang, J. D-shaped plastic optical fber sensor for testing refractive index. IEEE Sensors J. 14, 1673–1676 (2014).